

that the recombination were nondissociative then the value of  $\alpha_m$  given above would have to be increased by a factor of 2. The importance of the dissociative recombination mechanisms under appropriate conditions in the noble gases is widely accepted.<sup>21</sup> While it is probable that molecular cesium recombines dissociatively, it is not certain. The large values of cesium recombination observed by Dandurand and Holt<sup>22</sup> ( $3\text{--}12 \times 10^{-7}$  cm<sup>3</sup>/sec) at around 300°K are due to molecular recombination although Dandurand and Holt attribute their observation to a nondissociative mechanism. Very recently Harris<sup>23</sup> reported a value of cesium molecular recombination of  $10^{-8}$  cm<sup>3</sup>/sec in the temperature range 1520–1670°K. He definitely attributes his observation to dissociative recombination. Bates<sup>24</sup> has made a rough estimate of dissociative recombination and predicts values of the order of  $10^{-7}$  cm<sup>3</sup>/sec at  $T=250^\circ\text{K}$ . The temperature dependence of the coefficient that Bates gives is roughly as  $1/\sqrt{T}$ . By Bates'

<sup>21</sup> D. R. Bates, *Atomic and Molecular Processes* (Academic Press Inc., New York, 1962), p. 266.

<sup>22</sup> P. Dandurand and R. B. Holt, *Phys. Rev.* **82**, 278 (1951).

<sup>23</sup> L. P. Harris, *J. Appl. Phys.* **36**, 1543 (1965).

<sup>24</sup> D. R. Bates, *Phys. Rev.* **77**, 718 (1950); **78**, 492 (1950).

estimate, then, the coefficient at  $T=1380^\circ\text{K}$  would be  $4 \times 10^{-8}$  cm<sup>3</sup>/sec. Thus, both the recent experimental work of Harris and the estimate of Bates agree with the experimental value found by the beam method for the molecular recombination. The Dandurand and Holt values are, however, at least an order of magnitude larger than those found in this experiment. It seems likely, however, that the high values of recombination observed by all of the measurements on cesium molecular ions are due to dissociative recombination.

#### ACKNOWLEDGMENTS

The authors wish to thank Professor B. Bederson of New York University for much helpful discussion and advice. We are indebted to Dr. S. Bloom of RCA Laboratories for his continued encouragement and his critical reading of the manuscript.

The help of P. V. Goedertier and J. J. Thomas of RCA Laboratories during the earlier stages of the program is gratefully recognized.

The complex assembly operations required in this experiment were ably performed by N. Klein and R. Chamberlain.

## Absolute Cross Sections for Single Ionization of Alkali Ions by Electron Impact. I. Description of Apparatus and Li<sup>+</sup> Results\*

W. C. LINEBERGER,† J. W. HOOPER, AND E. W. MCDANIEL

*Georgia Institute of Technology, Atlanta, Georgia*

(Received 19 August 1965)

The absolute cross sections for the single ionization of Li<sup>+</sup> ions by electron impact have been measured over the electron-energy range from below threshold (75.6 eV) to 800 eV. The measurements were performed with an ultrahigh-vacuum crossed-beam facility operating under continuous, rather than the usual time modulated, beam conditions. A detailed description of the apparatus and experimental method is presented. Numerous checks were performed to justify the use of the continuous-beam measurement technique developed for this experiment, particular attention being paid to beam intensities, beam profiles, space charge, signal-to-noise ratio, and ion-beam composition. The error in the measured cross sections is believed not to exceed  $\pm 12\%$  above 150 eV electron energy; it may be as large as  $\pm 21\%$  at 90 eV. Of this possible error, an amount  $\pm 6\%$  is considered systematic.

### I. INTRODUCTION

ELASTIC and inelastic collisions involving electrons and heavy particles are of great importance in astrophysics, upper atmospheric phenomena, thermonuclear research, plasma physics, and gaseous electronics. Experimental information concerning such collisions may be obtained either indirectly from swarm studies

or directly from beam experiments. The vast majority of direct-collision studies have involved the passage of a beam of projectiles through a target gas, and either detection of the reaction products formed in the gas or observation of changes in the composition of the emerging beam. However, the single-beam approach is not applicable to the study of many of the reactions of greatest interest—for example, those between two species of charged particles. To obtain reliable results in such cases, it is usually necessary to study collisions occurring in intersecting beams.

This paper describes the experimental apparatus and techniques employed for the measurement of the cross

\* This work was partially supported by the Controlled Thermonuclear Research Program of the U. S. Atomic Energy Commission.

† The work reported here is a portion of a research program undertaken by one of us (WCL) in partial fulfillment of the requirements for the degree of Doctor of Philosophy at the Georgia Institute of Technology.

sections for single ionization of  $\text{Li}^+$  ions by electron impact over an electron energy range from below threshold (75.6 eV) to 800 eV. The following paper<sup>1</sup> (Paper II) reports measurements of electron-impact ionization of  $\text{K}^+$  and  $\text{Na}^+$  ions by electron impact, and contains the comparisons of all of the data with relevant theory and experiment.

The present measurements were performed with a crossed-beam apparatus operating under continuous-beam conditions. The experimental method involves intersecting approximately monoenergetic beams of lithium ions and electrons in a well-defined collision volume. The energy of the primary  $\text{Li}^+$  ions is set to be large compared with the energy change experienced by any of these ions in elastic scattering, ionization, or charge-transfer events, but their velocity will be low enough that the relative velocity of the two beams is essentially equal to the velocity of the electron beam in the laboratory frame of reference. There are no appreciable electric or magnetic fields in the beam intersection region. Therefore, all of the projectile ions, including those which undergo reactions either with electrons or with background gas molecules, travel essentially the same trajectory until the ion beam is separated into its various charge states after passage through the intersection region. Measurements of the composition of the final lithium beam will yield the absolute ionization cross section for the  $\text{Li}^+$  projectiles, provided that the geometries and intensities of the ion and electron beams are known and provided that the effects of the background gases are properly assessed. The present research represents the first successful absolute measurements of the cross sections for ionization of ions by electron impact in which the particle beams were operated continuously instead of being modulated in time. The utilization of ultrahigh-vacuum techniques was a primary factor enabling the use of continuous beams.

Only with the recent improvements in vacuum technology and development of pulsed-beam techniques<sup>2,3</sup> has it become possible to obtain reliable results in crossed-beam experiments. Of those modulated, crossed-beam experiments which have been performed, the work of greatest relevance to that described here is the measurement of the cross sections for ionization of  $\text{He}^+$  ions by electrons in the energy range from 54.5 to 1000 eV. This experiment, performed in 1961 by Dolder, Harrison, and Thonemann,<sup>4</sup> was the first study made of the ionization of positive ions by electron impact. The same group has subsequently measured the ionization cross sections for electrons on  $\text{Ne}^+$ <sup>5</sup> and  $\text{N}^+$ .<sup>6</sup> In addition

<sup>1</sup> J. W. Hooper, W. C. Lineberger, and F. M. Bacon, following paper, *Phys. Rev.* **141**, 165 (1966).

<sup>2</sup> R. L. F. Boyd and G. W. Green, *Proc. Phys. Soc. (London)* **71**, 351 (1958).

<sup>3</sup> W. L. Fite and R. T. Brackmann, *Phys. Rev.* **112**, 1141 (1958).

<sup>4</sup> K. T. Dolder, M. F. A. Harrison, and P. C. Thonemann, *Proc. Roy. Soc. (London)* **A264**, 367 (1961).

<sup>5</sup> K. T. Dolder, M. F. A. Harrison, and P. C. Thonemann, *Proc. Roy. Soc. (London)* **A274**, 546 (1963).

<sup>6</sup> K. T. Dolder, M. F. A. Harrison, and P. C. Thonemann, *Proc. Phys. Soc. (London)* **82**, 368 (1963).

to this work, Latypov, Kupriyanov, and Tunistkii<sup>7,8</sup> have recently published measurements of the ionization cross sections for electrons incident on several species of ions.

## II. GENERAL ASPECTS OF CHARGED-PARTICLE-CHARGED-PARTICLE CROSSED-BEAM EXPERIMENTS

This section concerns some general features of charged-particle-charged-particle ionization experiments. An expression for the ionization cross section in terms of the experimental parameters is presented. The difficulties associated with these experiments are discussed and in this connection several criteria are set forth for evaluation of the performance of an experimental apparatus. Published data are briefly reviewed in the light of these criteria.

In an electron-ion crossed-beam ionization experiment beams of ions and electrons are caused to intersect in a collision region. As a consequence of the much greater mass of the ion, it is possible to ensure that any interaction with the electron beam results in small-angle scattering of the ions. Thus those ions which have undergone interactions with the electrons emerge from the collision region with essentially the same velocity as that of the unreacted ions. In the case of electron-impact ionization of the ions, the reacted component can be separated from the primary beam by means of either magnetostatic or electrostatic charge-state analyzers. The electron current, the currents of reacted and unreacted ions, and the various projectile energies are experimentally observed quantities from which the desired cross sections may be calculated.

Consider a monoenergetic electron beam and a monoenergetic singly charged ion beam traveling parallel to the  $X$  and  $Y$  axes, respectively, of a rectangular Cartesian coordinate system. Let  $V_i$  and  $V_e$  be the ion and electron velocities. If both beams are sufficiently tenuous that multiple collisions can be neglected, then it can be shown that the cross section for the second ionization of the ions is given by the equation,<sup>9</sup>

$$\sigma_{i2} = \frac{eV_iV_e}{2(V_i^2 + V_e^2)^{1/2}} \frac{I^{++}}{\int_{-\infty}^{\infty} i^+(z)j(z)dz}, \quad (1)$$

where  $i^+(z)dz$  and  $j(z)dz$  are the ion and electron currents passing through the region  $z$  to  $z+dz$ ,  $I^{++}$  is the total current of doubly charged ions produced by electron impact, and  $e$  is the magnitude of electronic charge.

<sup>7</sup> S. E. Kupriyanov and Z. Z. Latypov, *Zh. Eksperim. i Teor. Fiz.* **45**, 1815 (1963) [English transl.: *Soviet Phys.—JETP* **18**, 558 (1964)].

<sup>8</sup> Z. Z. Latypov, S. E. Kupriyanov, and N. N. Tunistkii, *Zh. Eksperim. i Teor. Fiz.* **46**, 833 (1964) [English transl.: *Soviet Phys.—JETP* **19**, 570 (1964)].

<sup>9</sup> This expression is derived in Appendix I (Paper II).

A more convenient form for this expression is

$$\sigma_{12} = \frac{I^{++}}{JI^{+}} \frac{eV_i V_e}{2(V_i^2 + V_e^2)^{1/2}} G, \quad (2)$$

where

$$G = I^{+} J \left/ \int_{-\infty}^{\infty} i^{+}(z) j(z) dz \right. \\ = \int_{-\infty}^{\infty} i^{+}(z) dz \int_{-\infty}^{\infty} j(z) dz \left/ \int_{-\infty}^{\infty} i^{+}(z) j(z) dz \right. \quad (3)$$

and  $I^{+}$  and  $J$  are the total projectile ion and electron currents. With the exception of the factor  $G$ , Eq. (2) involves only known or directly measurable experimental quantities. The factor  $G$  is a form factor depending upon the current-density distributions of the ion and electron beams; it may be evaluated approximately by the use of scanning slits on both beams. The most obvious way of doing this is shown in Fig. 1. The movable slit scanner may be completely removed from the beam region to permit measurement of the total currents  $I^{++}$ ,  $J$ , and  $I^{+}$ . The scanner may then be lowered across the beams, as shown in the figure, to allow measurement of the beam current distributions. It is important to note that the scanner provides beam profile information *near* but not *in* the collision region, and that its presence in the beam region essentially negates the space-charge influence of one beam upon the other.

In this experiment, the electron velocity  $V_e$  is much greater than the ion velocity  $V_i$ . Under this condition the relative velocity of approach of an ion and an electron is essentially the electron laboratory velocity; the total energy in the center-of-mass reference frame is very nearly equal to the laboratory energy of the electron. Since the cross sections should be a function of the total center-of-mass energy, the measured cross sections should remain practically constant as the ion energy is varied, provided that the electron energy is fixed. For a given electron energy the measured cross sections should also be independent of changes in the electron beam intensity, the ion beam intensity, and the form factor  $G$ . As will be seen in Sec. IIC, the variation of each of these parameters provides a valuable check on some aspects of the performance of the experimental apparatus.

The following remarks will pertain to experimental difficulties primarily associated with crossed-beam experiments. Thus many problems common to all atomic collision experiments will be omitted. Among those to be omitted are such topics as Faraday-cup efficiency, particle loss from beams, beam-energy distributions, and accuracy of the measurement instrumentation.

#### A. Low Reaction Rates

The fact that both beams are composed of charged particles imposes a space-charge restriction on the maxi-

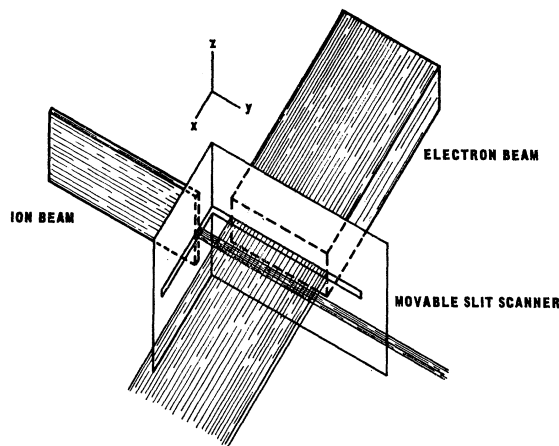


FIG. 1. Use of a movable slit scanner to determine beam profiles.

imum particle number density attainable in either beam. This restriction results in a severe limitation on the magnitude of the  $\text{Li}^{++}$  reaction component relative to those of the interacting electron and  $\text{Li}^{+}$  beams. Over the electron-energy range 50 to 500 eV, space-charge considerations limit the permissible electron current densities to the order of 1 mA/cm<sup>2</sup>. Such a current density represents an electron number density in the collision region which is far below the usual target number densities employed in single-beam experiments. This fact is responsible for the low reaction rates typical of charged-particle-charged-particle crossed-beam experiments. The measurements performed in the present research furnish a typical example. At an ion energy of 1 keV and with a 1.0 mA electron beam of 300-eV energy (an electron energy near the peak of the cross section), about 4  $\text{Li}^{+}$  ions in  $10^9$  are converted to  $\text{Li}^{++}$  ions. Thus the ion beam emerging from the collision region contains two components differing in intensity by about eight orders of magnitude. This difference in intensity requires that careful attention be paid to the ion-beam optics in order to prevent stray particles from the primary beam completely obscuring the smaller beam of the reaction product.

#### B. Interactions with Background Gas

Charged-particle-charged-particle crossed-beam experiments are further complicated by the fact that the number densities of the particles in the beams are comparable to the number density of the residual gases, even in an ultrahigh-vacuum ( $\sim 10^{-9}$  Torr) system. In general, the interaction of the primary ion beam with the residual gases cannot be ignored. In an electron ionization crossed-beam experiment the most troublesome of these interactions is that of charge stripping of the primary ion beam. Since charge stripping usually results in only a small deflection of the energetic ion, the charge-stripped ion may remain in the primary ion beam. If the stripping occurs in a field-free region near

the region of intersection with the electron beam, then the charge-stripped ion is indistinguishable from doubly ionized ions produced by electron impact.

The intensity of the charge-stripped component is directly proportional to the chamber pressure. Therefore, in order to determine the electron ionization component of the doubly charged beam, it is not necessarily sufficient to take the difference between  $I^{++}$  with the electron beam on and  $I^{++}$  with the electron beam off. In order for this difference to be a valid measure of the electron ionization component of the beam, assurance must first be made that either

- (1) the chamber pressure is unaffected by turning the electron beam "on" or "off," or
- (2) the charge-stripped component is sufficiently small relative to the electron ionization component that changes in the charge-stripped component attendant with turning the electron beam on and off do not make a significant difference in the computation of the net electron ionization current.

Requirement (1) can be met by pulsing the electron beam at a frequency sufficiently high that the chamber pressure cannot change appreciably between the "on" and "off" times of the pulses. A more useful approach, however, is to pulse both the ion and electron beams. By varying the relative phase of the two beams, they can be made to cross the collision region either in time coincidence or time anticoincidence. The difference between the  $I^{++}$  currents measured in these two modes yields the electron-impact-ionization current. Such a scheme has been employed in the experiments by Dolder, Harrison, and Thonemann.<sup>4-6</sup> This beam pulsing scheme and other possible techniques are considered in detail in Appendix II of Paper II.

Since the pressure will certainly rise when the electron beam is turned on, the difference between  $I^{++}$  with both beams on and  $I^{++}$  with only the ion beam on will be greater than the electron-impact-ionization current by an amount equal to the increase in the charge-stripped ion current produced by the pressure increase. It is possible, however, to assess whether a significant error results from assuming that the charge-stripping component of this difference measurement is much less than the electron-impact-ionization component. At electron energies below the threshold for electron-impact ionization of the ions, the electron-impact-ionization component of this difference measurement will be zero. The charge-stripping component is not a serious source of error provided that the difference measurement below threshold yields a result which is insignificant compared with that found well above threshold. This statement assumes, of course, that the below threshold measurements are made with ion and electron-beam intensities which are typical of measurements above threshold. The ratio of the charge-stripped current to the electron-impact-ionization signal depends upon the electron

beam intensity, the ratio of the stripping cross section to the ionization cross section, the geometry of the apparatus, the angular distribution of the charge-stripped ions, and the residual gas pressure. In order for the charge-stripping component not to be a serious source of error, and thus for cross sections to be able to be measured without the use of pulsing techniques, it will generally be necessary to reduce the operating pressure of the experimental apparatus to  $10^{-8}$  Torr or lower. Provided only that the measured cross section is zero below threshold, this continuous beam-measurement scheme is equal or superior to any pulsing scheme, as discussed in Appendix II of Paper II.

### C. Space Charge and Beam Profiles

As indicated previously, the absolute measurement of the cross section requires knowledge of the current-density distributions of the intersecting beams. Some form of beam scanner must be employed to obtain this information, from which the form factor  $G$  may be calculated. The form-factor determination is subject to error from two principal sources, namely: (1) The profile determinations are made a short distance away from the beam-intersection region rather than within this region, and (2) the beam profiles determined with the scanner may not reflect the alterations in the beam profiles at the intersection region which are produced by the macroscopic space-charge influence of one beam upon the other. We shall now consider errors in form-factor determination resulting from each of these sources, and formulate checks for the presence of these possible errors. Finally, criteria will be developed for determining when the beam profiles are satisfactory.

The fact that the scanner is located away from the interaction region permits form-factor errors resulting from space-charge expansion of the beams and from tilt of the beams. If, in Fig. 1, either beam is not traveling exactly parallel to the  $X$ - $Y$  plane, then the relative positions of the current-density distributions as determined by the scanner are not the same as their relative locations at the interaction region. It is therefore desirable to be able to show that the form remains unchanged upon translating one of the measured profiles a small distance  $\pm \Delta z$  with respect to the other. A large tilt in one of the beams can be detected in the following manner: The scanning slit is set to a central position in the beam-current distributions, thereby restricting the heights of the ion and electron beams to that of the scanning slit. A check is made to determine whether any electron-impact-ionization signal is present. Provided that any such signal can be detected, the approximate relative shift in the beam profiles is less than the height of the scanner slit. In this case, the form factor need be invariant only for a relative profile shift of  $\pm h$ , where  $h$  is the height of the scanner slit.

Both beams will expand as a result of their space charge. The electron-beam expansion will generally be

much greater than that of the ion beam, as a consequence of its normally much greater space charge. The electron-beam height observed with the scanner will consequently be somewhat less than the actual electron-beam height at the interaction region. In order to avoid errors arising from this source, the ion beam should be taller than the electron beam. If the ion beam is both reasonably uniform and taller than the electron beam, then the measured form factor will be close to the actual form factor, namely that for a somewhat "spread out" electron beam. This point can be checked by simply calculating the form factor for an electron-beam profile which has been altered to simulate space-charge spread, and verifying that the resulting form factor is the same as the form factor obtained for the unaltered beam. Since the space-charge spread of the electron beam is proportional to the electron-beam intensity, this point can also be checked by verifying that the measured cross section is independent of the electron-beam intensity. When the ion and electron beams are of the same height, significant errors will almost surely arise from this source.

In addition to these self-space-charge effects, the space-charge influence of one beam upon the other can create errors in profile determination. The electron-beam number density is both large and also much greater than that of the ion beam; consequently the electron beam can significantly influence the ion beam, whereas the effect of the ion beam upon the electron beam is small. For example, if there are losses from the ion beam resulting from divergence in the  $z$  direction with no electron beam, then the presence of the electron beam can reduce or eliminate these losses. The ion beam tends to move to those regions where the electron beam is most dense. Since the scanner blocks off most of both beams, this space-charge interaction is not reflected in the measured profile. This difficulty is not eliminated by simply having an ion beam whose measured profile is both uniform and taller than that of the electron beam. Such a beam will still develop a more dense region in the vicinity of the electron beam, and the measured profile will be in error. The ion deflection is not serious, however, if it can be shown that the measured cross section is independent of ion energy. Since the ion deflection is reduced as the ion velocity increases, constancy of the measured cross sections as the ion energy is varied implies that deflection of the ion beam by the electron space charge is not significantly affecting the measured beam profiles.

The question naturally arises as to what characterizes a "good" beam profile. Other workers<sup>4</sup> have defined a form factor in the following manner. Let both beams be restricted by apertures to the range  $0 \leq z \leq h$ . Then, after multiplication and division by  $h$ , Eq. (2) may be rewritten as

$$\sigma_{12} = \frac{I^{++}}{I+J} \frac{heV_i V_e}{2(V_i^2 + V_e^2)^{1/2}} F, \quad (4)$$

where

$$F = \frac{\int_0^h i^+(z) dz \int_0^h j(z) dz}{h \int_0^h i^+(z) j(z) dz}. \quad (5)$$

The form factors  $G$  and  $F$  differ only trivially. However, the expression for the cross sections which employs the form factor  $F$  appears to depend on the height of the beam-defining apertures,  $h$ . Such a dependence, of course, does not exist, but the appearance of  $h$  in the cross-section expression can be misleading. In order to avoid this possible confusion, the first expression for the cross section will be employed here. We note that if either beam is uniform, the form factor  $F$  is equal to unity. Unfortunately, a form factor of unity does not ensure "good" profiles because any of the following problems might still be present.

(1) The ion and electron beams might be of the same height, thus yielding errors as a result of space-charge spread of the electron beam.

(2) The convergence of the ion by the electron beam is not assessed. It still remains to be shown, as an additional check, that the measured results are independent of ion energy.

(3) The beams may not be uniform. There exist grossly nonuniform beams for which the form factor  $F$  is unity.

The conclusion is, therefore, that a single number cannot be used as a measure of the quality of the beam profiles. A better scheme is to regard the form factor as a functional defined on the ion- and electron-beam current-density distributions,  $i^+(z)$  and  $j(z)$ , respectively. A "good" profile is then one whose form factor is relatively constant with respect to certain variations in  $i^+(z)$  and  $j(z)$ . These variations are those which arise from or simulate tilt and space-charge spreading of the electron beam. In addition, the measured cross sections must be independent of ion energy. If these criteria are met, then the beam profiles can be said to be "good." It is perhaps worth noting that the effects mentioned in this discussion are not too small ever to be noticed; it has been possible to observe each of them in the experimental apparatus described in this paper.

#### D. Excitation State of Ion Beam

In order for an experiment to yield unambiguous results it is necessary to know the state of excitation of the ion beam. The only significant contamination will usually arise from metastable states, since the ion source can be sufficiently removed from the interaction region to permit the decay of ordinary excited states before the interaction occurs. Metastable contamination is, however, a serious problem, for in an ionization experiment the cross section for ionization of a metastable ion is expected to be much greater than that of the ground-state ion. However, the threshold energy for

ionization of the metastable ion lies below that of the ground-state ion. Therefore, the presence of significant metastable-ion contamination can be readily determined by measuring the ionization cross section at an electron energy just below the ground-state ionization threshold but above the metastable-state ionization threshold. If the resultant cross section is zero to within the experimental error, then any metastable component of the primary ion beam does not present a serious problem. In this connection thermionic-ion sources are to be preferred over electron-impact sources, since the thermionic emission process<sup>10</sup> precludes the emission of appreciable numbers of ions in excited states.

### III. CRITIQUE OF CHARGED-PARTICLE-CHARGED-PARTICLE CROSSED-BEAM RESEARCH

In the preceding section, a number of difficulties present in crossed-beam experiments have been discussed. From these difficulties emerge several criteria which can be utilized to assess the validity of a crossed-beam experiment. These criteria are summarized below.

- (1) The measured cross sections should be independent of the electron-beam intensity.
- (2) The measured cross sections should be independent of the ion-beam intensity.
- (3) The measured cross sections should be independent of changes in the beam profiles.
- (4) The measured cross sections should be independent of changes in the ion-beam energy.
- (5) The measured cross sections should ideally be zero below the threshold energy for the process being studied. If this is not the case, then a plausible explanation for the nonzero result must be given, together with a means for extracting the desired cross section from the actual measurements.
- (6) If beam-pulsing techniques are not utilized, then it must be demonstrated that ion-beam interactions with the residual gases were properly taken into account.

As of this date two groups have published results of charged-particle-charged-particle crossed-beam experiments. These groups are Dolder, Harrison, and Thonemann<sup>4-6</sup> at the Atomic Energy Research Establishment in England, and Latypov, Kupriyanov, and Tunitskii<sup>7,8</sup> at the L. Ya Karpov Physico-Chemical Institute in the Soviet Union. The pulsed-beam measurements of Dolder *et al.*, appear to satisfy all of the above criteria. The measurements of Latypov *et al.*, however, do not satisfy several of the criteria, and it is likely that large errors are present in their measurements. These publications are discussed in more detail elsewhere.<sup>11</sup>

<sup>10</sup> E. W. McDaniel, *Collision Phenomena in Ionized Gases* (John Wiley & Sons, Inc., New York, 1964), Chap. 13.

<sup>11</sup> W. C. Lineberger, J. W. Hooper, and E. W. McDaniel, Technical Progress Report No. 8 U. S. AEC Contract No. AT-(40-1)-3027, Georgia Institute of Technology, Atlanta, Georgia, 1965 (unpublished). (Available from authors on request.)

### IV. EXPERIMENTAL APPARATUS

A schematic diagram of the experimental apparatus is presented in Fig. 2. In the diagram the beam scanner, which intercepts the ion and electron beams just prior to their intersection, is not visible. In addition, the ion-source details and the extensive shielding of the Li<sup>++</sup> Faraday cup have been omitted for clarity. The remainder of this section consists of a description of the principal components of the experimental apparatus.

The vacuum enclosure is an all stainless-steel bakable chamber 21 in. in diameter and 6 in. high. It is pumped by a 4-in. oil diffusion pump with a water-cooled baffle and a zeolite trap to reduce backstreaming. The vacuum seals are the type where a soft aluminum wire is compressed between two flat surfaces. This gasket design is similar to that discussed by Holland and co-workers.<sup>12-15</sup> The base pressure in this system is about 10<sup>-9</sup> Torr; with ion and electron sources operating the indicated chamber pressure is about 10<sup>-8</sup> Torr.

#### A. Ion Emitting Material

The source of Li<sup>+</sup> ions is a platinum-gauze filament coated with  $\beta$ -eucryptite, Li<sub>2</sub>O·Al<sub>2</sub>O<sub>3</sub>·2SiO<sub>2</sub>. Upon heating to 1100°C, Li<sup>+</sup> current densities of as much as 1 mA/cm<sup>2</sup> are available from  $\beta$ -eucryptite. This material and other thermionic-ion emitters were investigated by Blewett and Jones<sup>16</sup>; details of the preparation of synthetic  $\beta$ -eucryptite are given by Allison and Kamegai.<sup>17</sup>

For the present crossed-beam experiment, it is desirable to use an ion source which is free from contamination of other alkali ions. An appreciable sodium- or potassium-ion contamination of the ion beam cannot be tolerated, as the cross sections for electron-impact ionization of these ions are ten to twenty times larger than the corresponding cross sections for lithium ions. Beam purity considerations dictated the selection of synthetic  $\beta$ -eucryptite. Furthermore, in order to obtain a single-ion velocity it was decided to prepare the  $\beta$ -eucryptite from lithium compounds enriched in the mass-7 isotope.

Mass spectrographic analyses were made of the ion emission from the isotopically purified  $\beta$ -eucryptite. Upon initial heating to 1000°C, it was found that 98% of the total emission consisted of sodium and potassium ions, the latter comprising 60% of the total. This large contamination is a transient phenomenon, since after approximately 5 h of operation at 1000°C, lithium ions constitute more than 99.9% of the total emission. Moreover, the mass-7 lithium isotope represented 99.7% of the total lithium emission. It was found that this source,

<sup>12</sup> L. Holland, *J. Sci. Instr.* **38**, 339 (1961).

<sup>13</sup> J. Holden, L. Holland, and L. Laursen, *J. Sci. Instr.* **36**, 281 (1959).

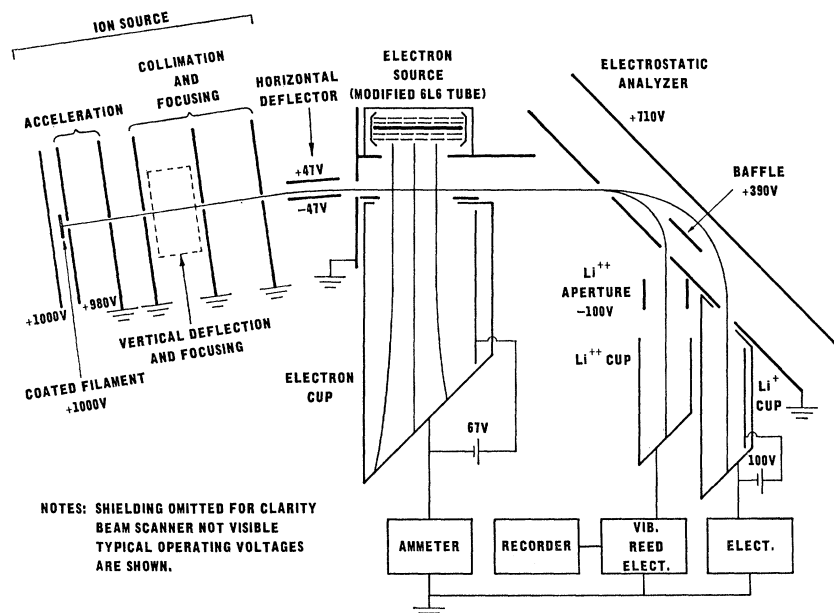
<sup>14</sup> L. Elsworth, L. Holland, and L. Laursen, *J. Sci. Instr.* **37**, 449 (1960).

<sup>15</sup> W. Steckelmachen, *Vacuum* **12**, 109 (1962).

<sup>16</sup> J. P. Blewett and E. J. Jones, *Phys. Rev.* **50**, 464 (1936).

<sup>17</sup> S. K. Allison and M. Kamegai, *Rev. Sci. Instr.* **32**, 1090 (1961).

FIG. 2. Schematic diagram of the experimental apparatus. The operation of each component is explained in the text.



operating at  $1000^{\circ}\text{C}$  and having an emitting area of approximately  $0.5\text{ cm}^2$ , could be relied upon to deliver  $10\ \mu\text{A}$  for at least 100 h. Source failures were generally a result of filament burnout, rather than depletion of the emitting material. Since source lifetime was quite adequate for this experiment, no attempt was made to optimize this parameter. The purity of the emitted ion beam obviated the necessity for including mass analysis within the cross-section apparatus.

### B. Ion Source and Optics

The ion source is of planar construction and produces a rectangular ion beam having a  $\frac{1}{4}\text{ in.} \times \frac{1}{32}\text{ in.}$  cross section. The general configuration and typical electrode voltages are indicated in Fig. 2. Beam definition in the  $\frac{1}{32}\text{-in.}$  dimension is obtained primarily by means of collimation. A pair of vertical deflection and focusing plates are located as shown in Fig. 2. The plates extend 1 in. along the beam flight path and are separated by  $\frac{3}{8}\text{ in.}$  The voltage applied to these plates is kept sufficiently low that the ion-beam deflection is less than 2 deg. The vertical focusing structure enables adjustment of the ion beam such that losses from the beam may be held to a negligible quantity (less than  $\frac{1}{2}\%$ ). This feature is essential, if one wishes to obtain meaningful results in this experiment. The vertical-deflection feature enables important checks to be made on the accuracy of beam profile determination. It is possible to make changes in the ion-beam shape and location relative to the electron beam, so that the form factor  $G$  can be varied while all other parameters are kept constant. It is imperative that the apparatus be adjusted such that the measured cross sections are independent of modest changes in the form factor introduced in this manner.

The horizontal deflector plates were introduced to eliminate a different problem. It was found that the  $\text{Li}^+$  beam contained a small component, about one part in  $10^8$ , which had either lost energy or been charge-stripped in collisions with the knife edges of the collimating slit in the ion source. Some of these ions can travel directly into the  $\text{Li}^{++}$  detector, when the ion-source geometry is linear. If, however, a small deviation in the ion beam is introduced electrostatically, then that portion of this component which had previously entered into the  $\text{Li}^{++}$  detector now suffers twice as much deflection as the main beam. The horizontal deflector introduces an 8-deg bend in the main ion beam, following the last slit edge that the ion beam is allowed to strike. The bend is sufficient to prevent the unwanted component from entering the post-interaction analyzer, and thus eliminates this cause of stray current to the  $\text{Li}^{++}$  detector.

The ion source is capable of delivering  $1.5\ \mu\text{A}$  of well-focused lithium ions at 1-keV energy. For this experiment the source is generally operated near  $2 \times 10^{-7}\text{ A}$  to provide a lower pressure and longer lifetime. As expected, no evidence has been observed which suggests the production by the thermionic source of any ions in excited states.

### C. Electrostatic Analyzer

After transit through the electron beam, the ion beam, which now contains  $\text{Li}^+$  and  $\text{Li}^{++}$  ions traveling at the same velocity, must be separated into its various charge states. Since the  $\text{Li}^{++}$  component may be  $10^{-9}$  times the size of the  $\text{Li}^+$  beam, the separation must be performed very carefully in order to prevent stray particles from the  $\text{Li}^+$  component from obscuring the  $\text{Li}^{++}$  component. It is desirable to analyze the ion beam as near to the

interaction region as possible; the analyzer fields, however, must not penetrate into the beam-interaction region. Either electrostatic or magnetostatic analyzers could be used to effect this separation. For this application the electrostatic analyzer was considered superior to the magnetostatic analyzer, both from space considerations and the fact that the fringe fields of the electrostatic analyzer are more easily controllable.

Charge-state separation is accomplished by an inclined parallel-plate electrostatic analyzer, as shown in Fig. 2. The structure is a modification of an energy selector proposed by Yarnold and Bolton,<sup>18</sup> and elaborated upon by Harrower.<sup>19</sup> The ion beam enters the analyzer at an angle of 45 deg with respect to the plates. The singly and doubly charged ionic species are separated in the electric field of the analyzer and exit at angles of 45 deg into their respective Faraday cups. If the incident ionic beam is composed of projectiles occupying a small angular region  $\Delta\theta$  about  $\theta=45$  deg, then, to first order in  $\Delta\theta$ , both components of the beam are focused on their respective exit apertures. This angular refocusing plus the ability to produce large deflections in a small physical space, represent major advantages over the more conventional parallel-plate electrostatic energy analyzer.

The plates of the analyzer are separated by  $1\frac{5}{16}$  in., while the spacing between adjacent apertures in the grounded plate of the analyzer is 2.0 in. The aperture sizes are approximately  $\frac{3}{8}$  in.  $\times$   $\frac{3}{4}$  in.; the size is thus much greater than the nominal  $\frac{1}{16}$  in.  $\times$   $\frac{1}{4}$  in. size of the ion beam in this region. The analyzer plates are sufficiently large (5 in.  $\times$  9 in.) that end-field effects are well removed from the vicinity of the ion beams.

The baffle plate in the analyzer (see Fig. 2) is held at the value of the local equipotential and does not seriously disturb the uniform electric field of the analyzer. This plate serves as a physical barrier for the slow ions which, as a result of ionization and charge-transfer interactions of the  $\text{Li}^+$  beam with the residual gases, are produced along the path of the  $\text{Li}^+$  beam. In the absence of this baffle plate, the slow ions so formed directly above the  $\text{Li}^{++}$  beam exit aperture would be accelerated into the  $\text{Li}^{++}$  cup region. Consideration of the  $10^{-8}$  Torr chamber pressure, and typical cross sections<sup>20,21</sup> for these processes shows that the ions so formed which enter the  $\text{Li}^{++}$  beam opening are considerably more numerous than the expected current of  $\text{Li}^{++}$  ions. The use of the baffle plate eliminates this source of stray current to the  $\text{Li}^{++}$  cup.

In spite of the large openings into the analyzer, it performs very nearly as predicted under the assumptions of infinitely large parallel planes with vanishingly

small entrance and exit apertures. Performance tests show that there is a broad plateau of analyzer voltage over which both components of the ion beam suffer no losses in traversing the analyzer to their appropriate exit apertures. The baffle-plate voltage adjustment has been shown to be noncritical. Wide variations of the baffle-plate voltage with respect to the total analyzer voltage do not impair the performance of the analyzer.

#### D. Ion-Collection and Current-Measurement Systems

The design and operation of the  $\text{Li}^+$  measurement system is routine and presents few problems. The magnitude of the  $\text{Li}^{++}$  beam current, about  $10^{-15}$  A, requires that special precautions be taken, and special techniques be employed, if meaningful measurements are to be made. The next two sections discuss the collection and measurement systems for these two ion beam components.

##### 1. $\text{Li}^+$ Collection and Measurement System

As seen in Fig. 2, the  $\text{Li}^+$  Faraday cup is a deep cup with the surface being struck by the ion beam inclined with respect to the beam. The solid angle subtended by the entrance to the cup at the region where the ion beam strikes the cup is less than 1% of the total solid angle. In addition, secondary electron and reflected ion-suppression structures are incorporated into the cup, but it has been demonstrated that the cup is essentially 100% efficient in retaining secondary charged particles even when no voltages are applied to the suppression structures. While reflected  $\text{Li}^+$  ions did not impair the performance of this collector due to the geometry employed, it must be noted that energetic reflected  $\text{Li}^+$  ions are present in appreciable numbers. Brunée<sup>22</sup> finds a reflection coefficient of 0.16 for 1-keV  $\text{Li}^+$  ions incident on clean molybdenum surfaces; he further finds that the energy distribution of these reflected ions is essentially flat out almost to the primary ion energy. Thus energetic reflected ions are a factor which must be considered throughout the entire ion-beam flight path.

The  $\text{Li}^+$  beam current is measured with a Keithley Model 610R electrometer. The instrument calibration is frequently checked with a Gyra Model CS-57 current source. The accuracy of the  $\text{Li}^+$  current instrumentation is better than  $\pm 2\%$ .

##### 2. $\text{Li}^{++}$ Collection and Measurement System

The  $\text{Li}^{++}$  Faraday cup, as seen in Fig. 2, sits back from the analyzer, but its entrance aperture is still large with respect to the ion-beam size. The  $\text{Li}^{++}$  aperture serves to suppress secondary electrons from the  $\text{Li}^{++}$  cup, and to prevent slow electrons from passing through the analyzer to the  $\text{Li}^{++}$  cup. It should be noted that a slow electron can be attracted into the analyzer entrance, be accelerated to the analyzer high-voltage plate,

<sup>18</sup> G. D. Yarnold and H. C. Bolton, *J. Sci. Instr.* **26**, 38 (1949).

<sup>19</sup> G. A. Harrower, *Rev. Sci. Instr.* **26**, 850 (1955).

<sup>20</sup> J. Van Eck, F. J. deHeer, and J. Kistemaker, *Proceedings of the Fifth International Conference on Ionization Phenomena in Gases, Munich, 1961* (North-Holland Publishing Company, Amsterdam, 1962), Vol. I, p. 54.

<sup>21</sup> K. Bethge, *Z. Physik* **162**, 34 (1961).

<sup>22</sup> C. Brunée, *Z. Physik* **147**, 161 (1957).

and, if the electron is elastically reflected at the plate, be energetically capable of traversing the analyzer to the  $\text{Li}^{++}$  cup. Since operation of the electron source tends to fill the vacuum chamber with a "cold" electron gas, this source of stray current to the  $\text{Li}^{++}$  cup was a serious problem until the  $\text{Li}^{++}$  aperture was installed. It has been shown that this Faraday cup collects the  $\text{Li}^{++}$  beam component with essentially 100% efficiency. The 100% collection efficiency is demonstrated in the following manner. The magnitude of the  $\text{Li}^{++}$  beam component is too small and too masked in noise to permit a direct observation of small changes in this current, while suppression voltages are being varied. Consequently, it was necessary to investigate the collection efficiency by indirect methods. The electrostatic analyzer voltage was doubled, thereby deflecting the  $\text{Li}^+$  beam into the  $\text{Li}^{++}$  cup. Variation of suppression voltages could now easily show that the  $\text{Li}^{++}$  cup collected the  $\text{Li}^+$  beam with essentially 100% efficiency. There is, however, a possibility that the  $\text{Li}^{++}$  beam might not be collected with the same efficiency as the  $\text{Li}^+$  beam. In order to investigate this point, the ionization cross section at a fixed electron energy was measured as a function of the electrostatic analyzer voltage. There exists a wide plateau of this voltage over which the measured cross sections do not change detectably. Since the  $\text{Li}^{++}$  beam collection geometry changes appreciably as the  $\text{Li}^{++}$  beam is swept across the  $\text{Li}^{++}$  cup, and since the measured cross sections do not change appreciably in this process, it is very unlikely that the  $\text{Li}^{++}$  beam collection efficiency is less than 100%. This observation, coupled with the demonstrated 100% collection efficiency for  $\text{Li}^+$  ions, leads to the conclusion that the  $\text{Li}^{++}$  collection structure is essentially 100% efficient.

The magnitude of the  $\text{Li}^{++}$  current requires that the cup and its lead wire be carefully shielded from stray charged particles. The  $\text{Li}^{++}$  aperture, Faraday cup, and its lead are completely enclosed with the exception of the exit aperture of the analyzer through which the  $\text{Li}^{++}$  beam travels. In the  $10^{-15}$  A range all insulators must be considered as possible sources of leakage and spurious currents. Thus, for the steatite insulator which supports the  $\text{Li}^{++}$  aperture, the following requirements were found: (1) The insulator must be mechanically secured to a grounded structure, rather than the  $\text{Li}^{++}$  cup. (2) The insulator must be electrostatically shielded from the  $\text{Li}^{++}$  cup. Requirement (1) is readily seen from an estimate of the leakage current across the insulator upon application of a 100-V potential. The second requirement arises from the fact that, upon application of a potential across the insulator, transient currents with a time constant of hours flow through the insulator. These currents produce a time-varying electric field which can in turn induce a time-varying charge on the  $\text{Li}^{++}$  cup. The net result is a varying current to the  $\text{Li}^{++}$  cup with a time constant of hours. Electrostatic shielding of the insulator from the  $\text{Li}^{++}$  cup and its lead wire eliminates this effect.

The current to the  $\text{Li}^{++}$  cup is measured with a Cary Model 31 vibrating reed electrometer. The electrometer preamplifier head mounts directly above the  $\text{Li}^{++}$  cup vacuum feed-through connector. Since the vibrating reed electrometer is a high input impedance device, care must be exercised to keep the Faraday cup and its electrical lead carefully insulated from ground. Only high-quality alumina and sapphire insulators are allowed to come in contact with the  $\text{Li}^{++}$  cup and its lead. In this manner the leakage resistance from the cup to ground has been kept greater than  $5 \times 10^{13} \Omega$ , as indicated by a Keithley Model 610R electrometer. The output of the vibrating reed electrometer is fed into a 10-in.-Honeywell Electronik Model 15 potentiometric recorder, whose accuracy is 0.25%.

Two modes are available for measuring currents with the vibrating reed electrometer. In the first mode, the instrument measures the voltage drop produced by the unknown current across a known large resistance. This mode has the advantages of simplicity and direct read-out of the magnitude of the ion current, but, as will be seen subsequently, these advantages accrue at the expense of additional noise and reduced accuracy. In the second mode of operation, known as the rate-of-charge mode, the instrument indicates the instantaneous voltage developed across a known precision capacitor by the beam current. If the beam current is constant, then

$$I = \Delta Q / \Delta t = (\Delta V / \Delta t) C, \quad (6)$$

where  $C$  is the capacitance of the capacitor being charged by the current  $I$ , and  $\Delta t$  is the time interval over which changed by  $\Delta V$  volts. The beam current is thus determined by measuring the average time derivative of the output voltage of the vibrating reed electrometer, and multiplying by the capacitance of the precision capacitor. This method requires the use of a recorder, and a considerable amount of additional time is required in order to determine the magnitude of the ion currents but, for measurements below  $10^{-13}$  A, the improved accuracy completely justifies the additional effort and time involved in the rate-of-charge measurement.

The rate-of-charge mode permits routine evaluations of  $dV/dt$  to an accuracy of better than  $\pm 1\%$ , a very difficult accuracy to approach in the resistor mode of operation. In order to determine the current absolutely, it is necessary to know the capacitance of the charging capacitor. This capacitance was determined by measuring a known current from a precision current source in the rate-of-charge mode; the capacitance was found to be  $(1.00 \pm 0.03) \times 10^{-11}$  F. Since the accuracy with which the voltage derivative can be determined is usually better than 1%, an over-all error of  $\pm 3\%$  in the determination of currents to the  $\text{Li}^{++}$  cup is indicated.

#### E. Electron Source, Collection, and Measurement Systems

The electron source is a modified 6L6GC beam power tube. A beam power tube was chosen for the source

since it is designed to produce an approximately rectangular electron beam. Typical electron-beam dimensions of 1 in.  $\times$   $\frac{3}{16}$  in. were employed. The 6L6GC is prepared for use in the following manner. The tube basing and envelope are removed and the plate structure is cut back, exposing the cathode and grids. The remaining plate sections are bent into a position for spot welding to a mounting bracket. Operational and cathode activation procedures for the electron source are similar to those described elsewhere.<sup>23-26</sup>

The electron Faraday cup is similar in design to the Li<sup>+</sup> Faraday cup. It also efficiently retains secondary electrons with no suppression voltages applied. An aperture plate is placed in front of the electron cup; its design is such as to allow only electrons which have passed through the ion beam to enter the electron Faraday cup. During data collection, the current to this plate is always less than 0.5% of the total electron beam current.

The electron current is determined by measuring the voltage drop produced by the electron beam across a precision resistor. The estimated error in the electron-current determination is  $\pm 1.0\%$ . The approximate energy distribution of the electron beam was determined by retarding potential techniques; the electron beam energy distribution has a half-width of approximately 2 eV, centered approximately 3 eV below the indicated accelerating voltage.

#### F. Shielding and Stray Current Reduction

The necessity for reducing stray currents to the Li<sup>++</sup> detector to the lowest possible level has already been pointed out. Steps taken in this direction which have been previously mentioned include the use of the horizontal deflector, the analyzer baffle plate, the Li<sup>++</sup> aperture plate, and the complete shielding of the Li<sup>++</sup> detection system. In addition to these measures it was necessary to enclose the electron source, and to provide baffling against particles entering the electrostatic analyzer through its sides or top. These steps reduced the stray electron current to the Li<sup>++</sup> detector to a low but not negligible level. Further reduction in this stray electron current is achieved by means of external magnets located above the Li<sup>++</sup> detection region. This magnetic field acts as a partial shield against electrons entering several small holes in the Li<sup>++</sup> detector shielding structure. Properly located, these magnets produce a negligible field in the vicinity of the electron beam. That this externally produced magnetic field does not impair the performance of the experimental apparatus is as-

sured through frequent checks, as discussed in connection with the experimental procedures.

### V. EXPERIMENTAL PROCEDURES AND RESULTS

An important segment of the experimental procedure is concerned with obtaining the correct Li<sup>++</sup> electron-ionization signal from the several currents measured at the Li<sup>++</sup> detector. This matter is considered first, followed by discussions of the measurement procedures, checks for consistency, and the experimental results and probable errors.

#### A. Currents to Li<sup>++</sup> Detector

Currents measured at the Li<sup>++</sup> detector include components produced by the spurious collection of Li<sup>+</sup> ions and electrons from the two crossed beams; by charge stripping and electron-impact ionization of the Li<sup>+</sup> beam; and by contact and thermal potentials present in the Li<sup>++</sup> detector assembly. Several terms must be defined in order to describe these components concisely. The following definitions are employed:

(1)  $I_{\text{sig}}^{++}(I, e)$  is that current of electron-impact-produced Li<sup>++</sup> ions present when a Li<sup>+</sup> beam of  $I$  amperes and an electron beam of  $e$  amperes are present in the interaction region.

(2)  $I^{++}(I, e)$  is that current measured at the Li<sup>++</sup> detector with a Li<sup>+</sup> beam of  $I$  amperes and an electron beam of  $e$  amperes present.

(3)  $I^{++}(I, 0)$  is that current measured at the Li<sup>++</sup> detector with only a Li<sup>+</sup> beam of  $I$  amperes present.

(4)  $I^{++}(0, e)$  is that current measured at the Li<sup>++</sup> detector with only an electron beam of  $e$  amperes present.

(5)  $I^{++}(0, 0)$  is the small background current measured at the Li<sup>++</sup> detector with no beams present. This current is a leakage current driven by thermal and contact potentials.

Several assumptions are now made regarding these currents; if these assumptions be valid then it becomes possible to extract  $I_{\text{sig}}^{++}(I, e)$  from the other  $I^{++}$  currents above. After statement of these assumptions, and deduction of the resultant expression for the Li<sup>++</sup> electron-impact-ionization component, it is necessary to show that, within the stated experimental error, these assumptions are valid in the present experimental apparatus. The assumptions are the following:

(1)  $I^{++}(0, 0)$  represents a steady background current whose magnitude is independent of the presence or absence of either or both of the ion and electron beams.

(2) The quantity  $[I^{++}(I, 0) - I^{++}(0, 0)]$  represents a Li<sup>+</sup> beam noise component whose magnitude is unaffected by the presence or absence of the electron beam.

(3) The quantity  $[I^{++}(0, e) - I^{++}(0, 0)]$  is an electron current to the Li<sup>++</sup> detector, the magnitude of which is independent of the presence or absence of the ion beam.

<sup>23</sup> W. H. Kohl, *Materials and Techniques for Electron Tubes* (Reinhold Publishing Corporation, New York, 1960), pp. 556-557.

<sup>24</sup> *Tube Laboratory Manual* (Research Laboratory of Electronics, Massachusetts Institute of Technology, Cambridge, Massachusetts, 1956), 2nd ed., pp. 46-50.

<sup>25</sup> G. A. Haas and J. T. Jenson, Jr., *Rev. Sci. Instr.* **28**, 1007 (1957).

<sup>26</sup> G. A. Haas and J. T. Jenson, Jr., *Rev. Sci. Instr.* **30**, 562 (1959).

Under these assumptions, an expression for  $I^{++}(I,e)$  may be determined as follows:

$$I^{++}(I,e) = I_{\text{sig}}^{++}(I,e) + [I^{++}(I,0) - I^{++}(0,0)] \\ + [I^{++}(0,e) - I^{++}(0,0)] + I^{++}(0,0). \quad (7)$$

Simplifying this result and solving for  $I_{\text{sig}}^{++}$  yields

$$I_{\text{sig}}^{++}(I,e) = [I^{++}(I,e) - I^{++}(I,0)] \\ - [I^{++}(0,e) - I^{++}(0,0)], \quad (8)$$

which is the desired expression for the electron-impact-ionization component. It remains to be shown, however, that the assumptions leading to Eq. (8) are valid.

At an electron energy below the ionization threshold of  $\text{Li}^+$  (75.6 eV), the quantity  $I_{\text{sig}}^{++}(I,e)$  should be zero. The measured value can be nonzero for several reasons, including (1) the contamination of the  $\text{Li}^+$  beam with  $\text{K}^+$  and/or  $\text{Na}^+$  impurities; (2) the presence of  $\text{Li}^+$  ions in excited states; (3) an increase in the collected charge-stripped  $\text{Li}^{++}$  component, as a result either of the converging influence of the electron-beam space charge or of pressure changes resulting from turning on the electron beam; and (4) the nonvalidity of any of the three assumptions leading to Eq. (8).

It has been found that  $I_{\text{sig}}^{++}(I,e)$  is zero below threshold, to within 2% of typical values of  $I_{\text{sig}}^{++}(I,e)$  well above threshold. This result has been determined frequently for various electron currents, ion currents, and electron energies below threshold. The variety of conditions under which  $I_{\text{sig}}^{++}(I,e)$  is zero below threshold should suffice to show that none of the four mechanisms above are operative, for it is unlikely that two errors could be self-canceling over a variety of operating conditions. Further checks are possible, however, since of all the possible mechanisms for producing a nonzero  $I_{\text{sig}}^{++}(I,e)$  below threshold, *only* an error in the electron correction term  $[I^{++}(0,e) - I^{++}(0,0)]$  can lead to a negative value. Thus any possible cancellations of errors producing zero signal current must be associated with the electron-correction term. By means of small changes in the positions of the external magnets it is possible to introduce an order-of-magnitude change in the electron-correction term. The ionization signal current below threshold remains zero throughout such changes in the electron-correction term. Thus an accidental cancellation can be effectively ruled out as a possibility. It should be finally noted that the electron-correction term is *not* a linear function of electron current; this fact alone makes an accidental cancellation unlikely.

In addition to the changes in the electron-correction term, the measured signal current is found to be independent of changes in the magnitude of the background current  $I^{++}(0,0)$  and the ion-beam noise current  $[I^{++}(I,0) - I^{++}(0,0)]$ . The resulting conclusions are, therefore, that none of the four mechanisms discussed previously are operative, and that the three assumptions concerning the currents to the  $\text{Li}^{++}$  detector are valid.

## B. Measurement Procedures

Before cross-section measurements can be made, a number of preliminary adjustments of the apparatus are necessary. These preliminary adjustments are listed below, followed by a short explanation where necessary.

(1) Following completion of the vacuum chamber bakeout, it is necessary to wait approximately 48 h for the background current  $I^{++}(0,0)$  to decay and stabilize. Before this time, the background current is too large and insufficiently steady to permit accurate measurements; the primary sources of this current are thermal gradients, contact potentials, and stressed insulators. The remaining adjustments take place after this current has stabilized.

(2) The stray electron current to the  $\text{Li}^{++}$  detector is minimized by means of external magnets located near the detector portion of the vacuum chamber. The absence of appreciable stray magnetic fields in the interaction region is assured by observing the electron current to the electron-cup aperture plate at low electron energies ( $\sim 50$  eV). Since a small deflection of these electrons is sufficient to produce a significant current to the electron Faraday-cup aperture plate, the absence of such current assures that the effect of the external magnets in the interaction region is small.

(3) The voltages of the electrostatic analyzer and horizontal deflector are adjusted such that both the  $\text{Li}^+$  and  $\text{Li}^{++}$  beams are centered on their respective exit apertures in the electrostatic analyzer. The aperture sizes are sufficiently large that  $\pm 5\%$  changes in the electrostatic analyzer voltages do not affect either of these currents. Particle losses in the analyzer are checked by doubling the analyzer voltage, thus deflecting the  $\text{Li}^+$  beam into the  $\text{Li}^{++}$  detector. The electrostatic-analyzer and horizontal-deflector voltages are always adjusted such that the  $\text{Li}^+$  currents measured at these two detectors agree to within the accuracy of the measurement instrumentation.

(4) The  $\text{Li}^+$  beam is focused so as to restrict losses from the beam to less than 1.0%. Particle losses are determined by measuring the increase in ion-beam intensity resulting from application of the electron beam. The increase in ion-beam intensity usually saturates at a few milliamperes electron beam intensity. The ion-beam loss is taken to be the fractional increase in ion-beam intensity as the electron-beam intensity is increased from 0 to 10 mA.

(5) The ion-beam profile is adjusted by means of the vertical deflection structure so as to obtain a "good" form factor.

(6) A check is made to assure none of the currents measured at the  $\text{Li}^{++}$  detector are rapidly varying functions of analyzer voltage. Such a condition may exist if either beam passes too close to the edge of an aperture.

Since some of these adjustments are interrelated, it is necessary to recheck all of them after the initial ad-

justments are made, and perhaps to make some slight readjustments. On occasion it may be impossible to meet all of these requirements. For example, it has at times been impossible to obtain small  $\text{Li}^+$  beam losses without introducing an unacceptable ion-beam profile. This condition generally necessitates disassembly of the apparatus, and replacement of the thermionic-ion emitter. Once the preliminary adjustments have been satisfactorily completed, the cross-section measurements proceed. The following is the step-by-step procedure employed to obtain the ionization cross section at a particular electron energy, electron-beam intensity, and ion-beam intensity.

(1) The electron energy, ion-beam intensity, and electron-beam intensity to be utilized in the measurements are selected.

(2) The slit scanner is lowered across the beams, to provide data for calculation of the form factor  $G$ . The normal scanner increments are 0.020 in.

(3) The quantities  $I^{++}(I,0)$  and  $I^{++}(I,e)$  are measured sequentially. Normally three measurements of each of these currents are made using the rate-of-charge mode. The length of time utilized for each determination is approximately 40 sec.

(4) The quantities  $I^{++}(0,e)$  and  $I^{++}(0,0)$  are measured; each current is measured at least twice.

(5) From (3) and (4), respectively, average values are calculated for  $[I^{++}(I,e) - I^{++}(I,0)]$  and  $[I^{++}(0,e) - I^{++}(0,0)]$ . From these quantities an average  $I_{\text{sig}}^{++}(I,e)$  is determined using Eq. (8). The ionization cross section is then calculated by use of Eqs. (2) and (3).

The following are typical values of the above quantities, for 350-eV electron energy and 1000-eV ion energy.

$$\begin{aligned} I^+ &= 2.00 \times 10^{-7} \text{ A}, & I^{++}(I,0) &= 1.44 \times 10^{-15} \text{ A}, \\ J &= 2.00 \times 10^{-3} \text{ A}, & I^{++}(I,e) &= 2.22 \times 10^{-15} \text{ A}, \\ I^{++}(0,0) &= -0.65 \times 10^{-15} \text{ A}, & I_{\text{sig}}^{++}(I,e) &= 2.27 \times 10^{-15} \text{ A}, \\ I^{++}(0,e) &= -2.14 \times 10^{-15} \text{ A}, & G &= 0.565 \text{ cm}. \end{aligned}$$

The data are taken at randomly varied electron energies. In addition, the ion- and electron-beam intensities are periodically varied to assure that the measured cross sections are independent of these parameters. Many of the checks on performance of the apparatus are made at 500-eV electron energy and at an electron energy below threshold. Approximately one out of every five measurements is a repetition of one of these check points; this procedure enables frequent checks to be made on the apparatus performance.

### C. Possible Errors and Checks for Consistency

A number of checks must be made before proper operation of the apparatus is assured. The results of the checks presented here pertain to the performance of the experimental apparatus during those periods in which the experimental results can be considered valid.

It should be emphasized, however, that the consistency exhibited by these checks was not obtained every time the apparatus was operated. Each of the effects discussed in Sec. II has, at one time or another, been observed in the course of the checking procedure, and has necessitated appropriate corrective measures before valid results could be obtained.

Figures 3(a) and 3(b) show the dependence of the measured cross sections on electron- and ion-beam intensities, respectively, at an ion-beam energy of 1000 eV. The scatter in these results is well within the acceptable error of this experiment.

The measured cross section below threshold is zero, to within  $\pm 2\%$  of the 500-eV cross section. As stated previously, this result assures the validity of the continuous beam technique utilized in this apparatus, and as is shown in Appendix II of Paper II, indicates that the use of any beam modulation scheme would represent no improvement in the performance of the apparatus. In addition, this result precludes the possibilities of significant  $\text{Na}^+$  or  $\text{K}^+$  contamination of the  $\text{Li}^+$  beam; of the presence of significant numbers of  $\text{Li}^+$  ions in excited states; and of significant electron beam convergence of more widely scattered charge-stripped  $\text{Li}^{++}$

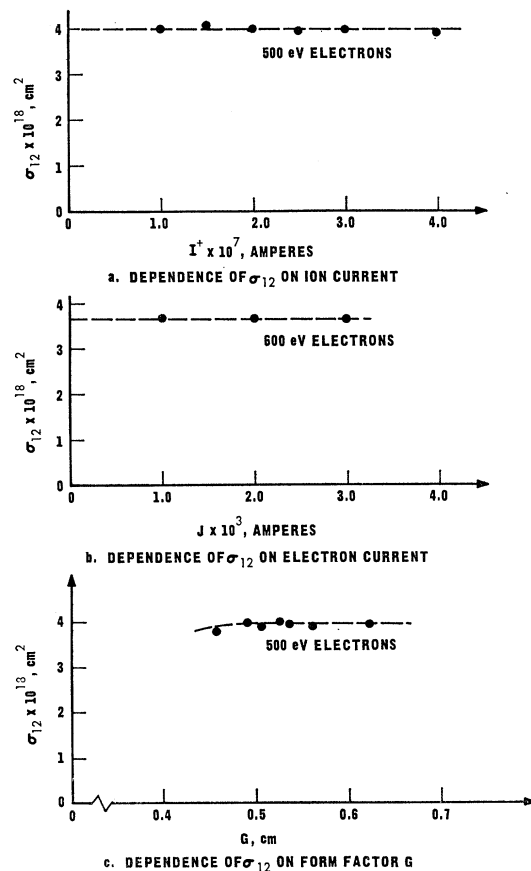
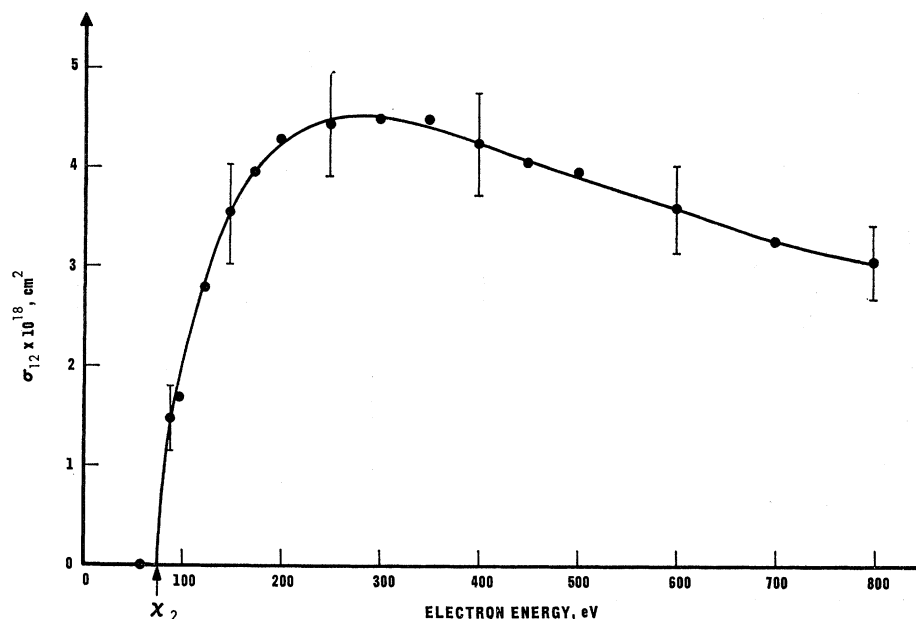


FIG. 3. Dependence of the measured cross sections on various experimental parameters.

FIG. 4. Absolute cross sections for the single ionization of  $\text{Li}^+$  ions by electron impact. The threshold energy for formation of  $\text{Li}^{++}$  ions is indicated by  $\chi_2$ .



ions. Thus obtaining a zero cross section below threshold represents one of the most important single checks on the operation of the apparatus.

It is necessary that the measured cross sections be independent of some changes in the beam profiles, and hence of changes in the form factor. This check is necessary to assure that the form-factor measurement does not introduce an appreciable error, as pointed out previously. Figure 3(c) depicts the variation of the 500-eV cross section with the form factor  $G$ , all other parameters being held constant. The ion beam is not perfectly uniform, and hence no simple interpretation can be given to  $G$ ; it can be said, however, that  $G$  is some sort of measure of the "height" of the ion beam. In fact, these variations in  $G$  were introduced by varying the vertical focus voltage and hence the "height" of the ion beam.

The cross section is essentially independent of changes in the form factor  $G$  except for the rolloff seen below  $G=0.47$ . These data were taken with electron-beam profiles which were nearly identical. The rolloff is thus a result of the ion beam becoming too small to accommodate the space-charge spreading of the electron beam. Were cross-section measurements made at  $G=0.45$  as a function of electron-beam intensity, it would be found that the measured cross sections would increase as the electron-beam intensity decreased. As is evident from Fig. 3(b), such is not the case when measurements are made with a value of  $G$  which is in the plateau portion of the curve. These facts, coupled with the observation that the 500-eV cross section is unaffected by increasing the ion-beam energy from 1000 to 1500 eV, indicate that no serious errors are present in the form-factor determination.

The measured cross sections are also shown to be

independent of small changes in the electrostatic-analyzer and horizontal-deflector voltages. As stated previously, the measured cross sections are independent of wide variations in  $I^{++}(0,0)$ ,  $I^{++}(0,e)$ , and  $I^{++}(I,0)$ . At the highest electron energies employed, 700 and 800 eV, the electron source occasionally tended to arc over from the control grid to the grounded screen grid. In order to avoid this difficulty, it was necessary to operate the screen grid at  $-100$  V when 700- or 800-eV electron energies were employed. There was a possibility of the screen-grid electric field penetrating appreciably into the interaction region. To investigate this point, the 500-eV cross section was measured as a function of screen-grid voltage over the range from 0 to  $-150$  V. No detectable variation in  $\sigma_{12}$  was observed, and it is concluded that the use of  $-100$  V on the screen grid at high electron energies introduces no appreciable error.

The same results have been obtained with several different ion and electron sources. Items such as the calibration of the measurement instrumentation and the efficiency of the Faraday cups have been discussed in the previous chapter.

#### D. Measurement Results and Discussion of Errors

The cross sections for single ionization of lithium ions by electron impact have been measured for electron energies over the range from below threshold to 800 eV. The results of these measurements are shown in Fig. 4, while the results are presented in tabular form in Table I.

The tabular data pertain to the actual measured cross sections, and not to the smooth curve which has been drawn as a "best fit" to the measured results. The maxi-

TABLE I. Absolute cross sections for the single ionization of  $\text{Li}^+$  ions by electron impact.

Indicated electron energy, eV	Actual electron energy, eV	$\sigma_{12} \times 10^{18}$ , $\text{cm}^2$	Random error, %	Maximum systematic error, %	Maximum total error, %
60	$57 \pm 2$	0.0	...	...	...
90	$87 \pm 2$	1.48	$\pm 15$	$\pm 6$	$\pm 21$
100	$97 \pm 2$	1.69	$\pm 10$	$\pm 6$	$\pm 16$
125	$122 \pm 2$	2.79	$\pm 10$	$\pm 6$	$\pm 16$
150	$147 \pm 2$	3.54	$\pm 8$	$\pm 6$	$\pm 14$
175	$172 \pm 2$	3.96	$\pm 6$	$\pm 6$	$\pm 12$
200	$197 \pm 3$	4.28	$\pm 6$	$\pm 6$	$\pm 12$
250	$247 \pm 3$	4.45	$\pm 6$	$\pm 6$	$\pm 12$
300	$297 \pm 3$	4.50	$\pm 6$	$\pm 6$	$\pm 12$
350	$347 \pm 3$	4.50	$\pm 6$	$\pm 6$	$\pm 12$
400	$397 \pm 3$	4.25	$\pm 6$	$\pm 6$	$\pm 12$
450	$447 \pm 3$	4.07	$\pm 6$	$\pm 6$	$\pm 12$
500	$497 \pm 3$	3.98	$\pm 6$	$\pm 6$	$\pm 12$
600	$597 \pm 4$	3.62	$\pm 6$	$\pm 6$	$\pm 12$
700	$697 \pm 4$	3.30	$\pm 6$	$\pm 6$	$\pm 12$
800	$797 \pm 4$	3.11	$\pm 6$	$\pm 6$	$\pm 12$

imum probable errors of the measurements are indicated by vertical bars on the graph, and are shown numerically in Table I.

The systematic errors arise primarily from instrumentation calibration errors; they are estimated to be a maximum of  $\pm 6\%$  at all electron energies. The random errors are more difficult to estimate for the following reason. Over short periods of time, repeated measurements of the cross section at 500 eV, for example, may exhibit very little scatter (less than  $\pm 2\%$ ). Over periods of weeks, however, wider variations are seen. These variations can usually be correlated with a deterioration of the degree to which the experimental apparatus satisfies the consistency checks, but it is felt that some weight must still be given to these variations. Accordingly, the random error is increased at 500 eV to  $\pm 6\%$ . At lower electron energies, where the short-term random error is larger, the total random error also is larger, as indicated in Table I. The estimated total possible error is taken to be the sum of the random and systematic errors. The total probable error in the measurements is thus believed not to exceed  $\pm 12\%$  above

150-eV electron energy; it increases at lower electron energies, and may be as large as  $\pm 21\%$  at 90 eV. The root-mean-square error, which is not shown, ranges from  $\pm 8\%$  at 800 eV to  $\pm 15\%$  at 90 eV.

In addition to these errors, there also exists some uncertainty in the mean electron energy in the interaction region. Retarding potential measurements show that the electron-energy spread is approximately  $\pm 2$  eV about the mean energy. The mean electron energy was determined in the following manner. Both retarding potential measurements and, subsequently, measurements of the electron-impact ionization of  $\text{K}^+$  ions near threshold were not inconsistent with the assumption that the mean electron energy was about 3 eV less than the indicated energy. Furthermore, the  $\text{K}^+$  measurements showed that the magnitude of this energy degradation must be less than 5 eV. An energy degradation of a few electron volts is typical of an oxide-coated cathode. For these reasons, the mean electron energy in the interaction region is taken to be 3 eV less than the indicated energy; the electron energy has been accordingly corrected in the data presented here. The electron energy is considered to be uncertain by  $\pm 2$  eV. This energy uncertainty has not been taken into account in determining the vertical error brackets. While the electron-energy uncertainty is insignificant at high energies, at low electron energies it must be considered. The uncertainty in the mean electron energy increases at higher energies, as a consequence of the 0.25% uncertainty in the indicated acceleration voltage. Comparisons of the  $\text{Li}^+$  cross sections with relevant theory and other experimental results are presented in the following paper (Paper II).

#### ACKNOWLEDGMENTS

We are pleased to acknowledge the expert assistance of F. M. Bacon during the later developmental phases of the apparatus and during the extensive data-collection process. Dr. R. A. Strehlow of the Oak Ridge National Laboratory prepared the isotopically purified  $\beta$ -eucryptite; for this service we are very grateful.